Control of higher spectral components by spatially inhomogeneous fields in quantum wells

Chaojin Zhang,[1,2] Chengpu Liu,[2,*] and Zhizhan Xu[2]

[1]*School of Physics and Electronic Engineering, Jiangsu Normal University, Xuzhou 221116, China*

[2]*State Key Laboratory of High Field Laser Physics, Shanghai Institute of Optics and Fine Mechanics, Chinese Academy of Sciences, Shanghai 201800, China*

(Received 22 April 2013; published 6 September 2013)

The propagation of a spatially inhomogeneous few-cycle laser field, linked to surface plasmon polaritons, through an ensemble of quantum wells is investigated under two conditions. It is found that the transmitted spectra sensitively depend on the spatial inhomogeneity due to the nonlinear propagation effects. Under the small-frequency mismatch condition, the transmitted spectral distribution is continuous for the spatially homogeneous case. However, when spatial inhomogeneity is introduced, the distribution is discrete instead, with clearly even- and odd-order harmonic peaks coexisting, which is related to the strong-field reshaping effect and the inversion symmetry breaking due to the introduction of the spatially inhomogeneous field. As for the large-frequency mismatch condition, only odd-order harmonics exist, no matter how strong the spatial inhomogeneity is. Under both conditions, the propagation effect can obviously enhance the intensity of higher spectral components.

DOI: 10.1103/PhysRevA.88.035805 PACS number(s): 42.65.Ky, 42.65.Re, 42.50.Md

I. INTRODUCTION

With the development of ultrafast laser technology, the laser pulse duration is down to a few cycles, and a series of new nonlinear optical effects have been found [1–9] when a few-cycle laser interacts with few-level atoms or molecules, such as the carrier-wave Rabi flopping [4,5], the third-harmonic generation in disguise of the second-harmonic generation [6], continuous or distinct features in transmitted spectra [8,9], and so on. In this regime, because of the advancement of computer-controlled molecular-beam-epitaxy technology, the investigations of few-cycle laser pulses interacting with semiconductor quantum wells have attracted considerable interest in recent years [10,11]. One advantage for a quantum well is that its width is adjustable, and therefore its electronic and optical properties can be controlled, which inversely affects the extreme nonlinear optical phenomena.

On the other hand, the surface plasmon polariton (SPP), induced when a laser field is irradiated on a given geometry of a nanostructure, has an important influence on the strong-field dynamics, which recently has attracted much more attention [12–14]. The field related to SPP is confined in narrowly localized regions and is not spatially homogeneous. Therefore it is naturally expected that obvious differences should exist between the two cases with and without field spatial homogeneity. The very recent investigations in high-order-harmonic generation [15–26] and above-threshold ionization [27–29] have confirmed this point. To our knowledge, however, no investigations are related to the propagation effects for such a field, especially for a few-cycle spatially inhomogenous field, for which the description in terms of slowly varying envelope and rotating wave approximations are not suitable [4]. It is very important, especially in cases of guiding local enhanced fields through subwavelength optical devices used in next-generation optical networks.

In this Brief Report, the propagation effect for such a field is investigated. The investigation is focused on what strong effect is induced and how the transmitted spectrum changes when a few-cycle spatially inhomogenous laser pulse propagates through an ensemble of square quantum wells. It is implemented under two conditions. First, when a small-frequency mismatch, i.e., near resonance between the laser frequency and the transition frequency of the quantum well, is met by adjusting the well width, it is shown that the spectra have a continuous feature in the higher spectral components for a spatially homogeneous field. However, for a spatially inhomogeneous field, the higher spectral components show a distinct feature and are obviously enhanced due to the propagation effect as well. Second, under the case of large mismatch, only the discrete feature is kept no matter whether the field is spatially homogeneous or not. After a detailed investigation, it is finally confirmed that the propagation effect is really important for the design and potential application of subwavelength optical devices.

II. THEORETICAL METHODS

The spatially inhomogeneous few-cycle laser field, after birth (usually via the surface-plasma-polariton mechanism in a dielectric-metal surface with subwavelength structures), propagates along the metal surface. What is interesting is what would be changed or induced when it propagates through a nonlinear medium, such as gases or semiconductor materials. Here we consider an ensemble of quantum wells as an example based on the consideration that as for a quantum well, as shown in Ref. [11], the well width a_0 is adjustable and, subsequently, the transition energy and transition moment are as well, which inversely affects the nonlinear properties. The interaction configuration between the few-cycle spatially inhomogeneous field and an ensemble of square quantum wells is shown in Fig. 1; the laser field propagates along the z direction with linear polarization along the x direction. The quantum well is simplified as a two-level system with one ground state and one excited state. The whole dynamics is determined by the

*chpliu@siom.ac.cn

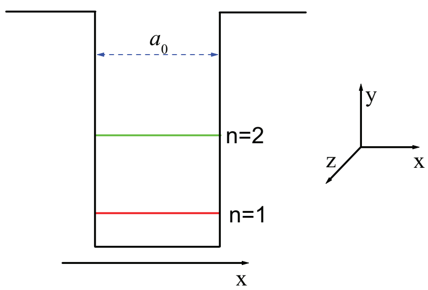

FIG. 1. (Color online) Conduction-band energy diagram for a square quantum well. Subband levels are labeled $n = 1$ and $n = 2$. a_0 is the width of the square quantum well.

Maxwell-Bloch equation group [30–32]:

$$\frac{\partial H_y}{\partial t} = -\frac{1}{\mu_0}\frac{\partial E_x}{\partial z}, \qquad \frac{\partial E_x}{\partial t} = -\frac{1}{\varepsilon_0}\frac{\partial H_y}{\partial z} - \frac{1}{\varepsilon_0}\frac{\partial P_x}{\partial t}, \tag{1}$$

$$\frac{\partial \rho_{12}}{\partial t} = -i\left(\omega_{12}\rho_{12} + \frac{E_x}{\hbar}un\right) - \frac{1}{\tau_1}\rho_{12}, \tag{2}$$

$$\frac{\partial n}{\partial t} = i\frac{2u}{\hbar}E_x(\rho_{12} - \rho_{12}^*) - \frac{1}{\tau_2}n, \tag{3}$$

where u is the transition matrix moment of the quantum well [11], ρ_{12} is the off-diagonal element of the density matrix, $n = \rho_{22} - \rho_{11}$ is the population difference between the excited and ground states, and $\hbar\omega_{12}$ is the transition energy of the system [11]. $P_x = 2Nu\text{Re}[\rho_{12}]$ is the macroscopic nonlinear polarization which connects with the off-diagonal element of the density matrix in the medium. Usually, the dephasing time τ_1 and the excited-state lifetime τ_2 are set to $\tau_1 = \tau_2 = 1$ ps [9]. The number density of the medium is taken to be $N = 6.0 \times 10^{22}\ \text{m}^{-3}$. The full-wave Maxwell-Bloch equations are solved by employing Yee's finite-difference time-domain (FDTD) discretization scheme [33–41].

Similar treatments can be found in many works [10,37,40]. The pulse initially propagates in the free space, and then it partially penetrates into the medium and partially reflects backwards; the penetrating part propagates through the medium and finally exits again into the free space. At exit, via Fourier transformation, we can get the field distribution in the frequency domain, i.e., the so-called transmitted spectra. The initial input field is written as [14,27]

$$E_x(t = 0, z) = E_0 \,\text{sech}\,[1.76(z/c - z_0/c)/\tau_0]\,[1 + \varepsilon h\,(x)] \times \sin\,[\omega_0(t - t_0)]\,, \tag{4}$$

where E_0 is the electric-field amplitude. ω_0 denotes the angular frequency of laser pulse. τ_0 is the full width at half maximum (FWHM) of the pulse intensity envelope. The choice of z_0 ensures that the pulse penetrates negligibly into the medium at $t = 0$ [37]. ε is called the inhomogeneous factor, which characterizes the laser-field inhomogeneity degree. $h(x)$ represents the functional form of the inhomogeneous field. Such a spatially inhomogeneous electric field is numerically obtained via the finite-difference time-domain algorithm, as shown in Refs. [14,27], but for simplicity and convenience of use, it is approximated using a power series $h\,(x) = \Sigma_{i=1}^{N} b_i x^i$, where the coefficients b_i are obtained by fitting the real electric field that results from a finite-element simulation. In the region relevant to the strong-field physics and electron dynamics, the electric field can be, indeed, approximated by a simple form for $h(x)$ [i.e., the linear term $h(x) = x$] [14,27]. Also we use the following laser parameters, which are similar to a previous report [4]: $\omega_0 = 0.0145$ a.u., $\tau_0 = 18$ fs, $z_0 = 42\ \mu$m. The incident pulse's area $A = 1.76E_0\tau_0\mu/\hbar = 4\pi$.

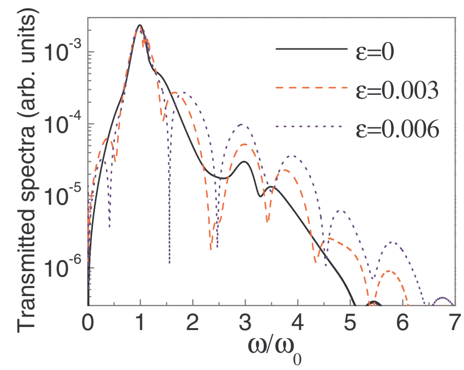

FIG. 2. (Color online) The transmitted spectra at different values of spatially inhomogeneous factor ε with a well width of 32.9 a.u. and propagation distance $z = 15.6\ \mu$m.

III. RESULTS AND DISCUSSION

First, the influence of the field spatial inhomogeneity on the transmitted spectra is studied. The quantum width of the square well is 32.9 a.u., and the laser frequency ω_0 has a small mismatch to the transition frequency ω_{12} (here $\omega_{12} = 1.11\omega_0$). The ensemble length is set as $z = 15.6\ \mu$m, and the results corresponding to the three field inhomogeneous factors ε are shown in Fig. 2.

If the field is spatially homogeneous, that is, $\varepsilon = 0$, the higher spectral distribution in the transmitted spectrum is almost continuous (solid line in Fig. 2), except for a barely visible oscillation around $3\omega_0$. This so-called third-harmonic component is well studied by Hughes [4] in a two-level atomic system, and he points out it comes from the incomplete carrier-wave Rabi flopping. A careful investigation of the transmitted spectral distribution as a function of the frequency mismatch (via changing the well width step by step; see the solid lines in Figs. 2, 5, and 6) indicates that the larger the mismatch is, the more obvious the third harmonic is.

For a spatially inhomogeneous case, however, even with a slightly weaker inhomogeneous factor $\varepsilon = 0.003$ ($\ll 1$), the spectral distribution becomes discrete. Clearly even or odd harmonics $(1, 2, 3, 4, \ldots)$ occur with the intensity exponentially decaying. It is worth pointing out that such a discrete spectral distribution is obtained in a symmetric quantum well system. Of course, this kind of distribution has been reported in an asymmetric system [7] or by using two-color ($\omega + 2\omega$) laser fields [8]. The occurrence of even-order harmonics here is also attributed to the broken inversion symmetry as usual, but the symmetry breaking is due to the introduction of the spatially inhomogeneous field in Eq. (4) [12].

More interestingly, when the spatially inhomogeneous factor ε increases to $\varepsilon = 0.006$, the spectral discrete peaks are evidently enhanced and also are more in contrast to the background noise (see dotted line in Fig. 2).

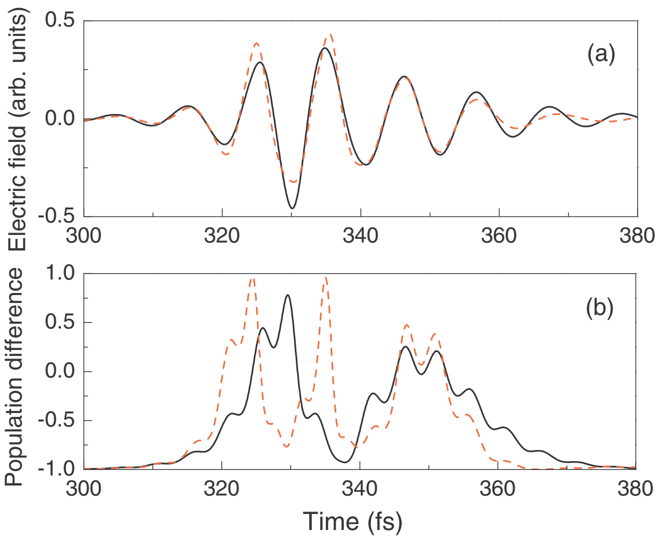

FIG. 3. (Color online) (a) The waveforms of the laser fields at different spatially inhomogeneous factors ($\varepsilon = 0$, solid line; $\varepsilon = 0.006$, dashed line) with a well width of 32.9 a.u. and propagation distance $z = 15.6\ \mu$m. (b) The corresponding population inversions.

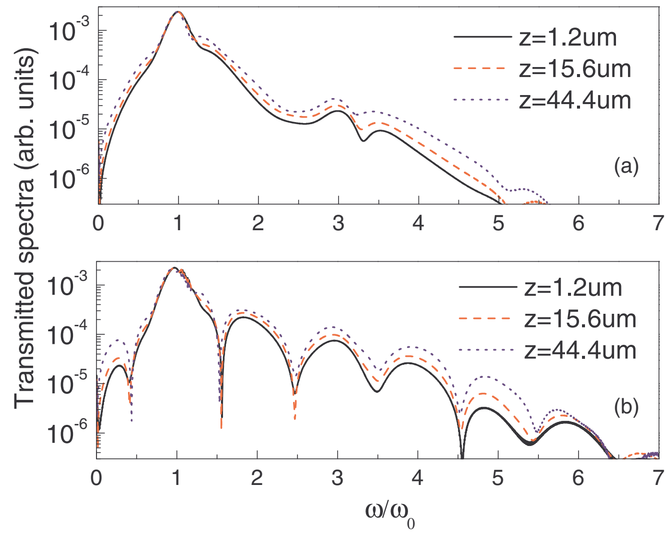

FIG. 4. (Color online) The transmitted spectra at different propagation distances in the (a) spatially homogeneous $\varepsilon = 0$ and (b) spatially inhomogeneous $\varepsilon = 0.006$ cases.

As for the reason why the spectral distribution becomes more discrete from the almost-continuous one in the case of a homogeneous field, clues can be drawn from the time evolution of the instantaneous laser field and the corresponding carrier-wave Rabi flopping shown in Fig. 3. As described in previous works [4,5], the incomplete carrier-wave Rabi flopping induces the higher and lower spectral components for a few-cycle laser pulse except for the fundamental frequency. When the spatial inhomogeneity is considered [see dashed line in Fig. 3(a)], after a short-distance propagation $z = 15.6\ \mu$m, the time profile of the electric field is reshaped, and its peak increases obviously. Of course, only the peak's increase introduced by the inhomogeneous factor in Eq. (4) does not result in the obvious increase of the higher spectral component, which is confirmed by the trivial change in the intensity for the laser's fundamental frequency, as shown in Fig. 2. By contrast, the enhancement of higher spectral components is really much more obvious. As for the spatially homogeneous case, there exist two incomplete carrier-wave Rabi floppings, and their interference results in the occurrence of higher spectral components [4,5]. Instead, when a spatially inhomogeneous field is introduced, the time profile of the electric field, due to a nonlinear interaction based on propagation, is strongly reshaped, and the first incomplete Rabi flopping is split into two, as shown in Fig. 3(b). These two floppings have almost comparable strength and a much smaller time delay between them, and therefore their strong interference results in the discrete higher spectral distribution.

The propagation effect is very important, as shown above, and one natural question occurs: what is the influence of the propagation distance? The transmitted spectra at different propagation distances in the two spatially homogeneous and inhomogeneous cases are shown in Fig. 4. From Fig. 4, the farther the laser propagates, the more significant the enhancement of the spectral strength is. Interestingly, in the spatially inhomogeneous case [Fig. 4(b)] under the same propagation distance change, the higher-frequency peaks increase more obviously (even by one order of magnitude). The higher-spectra peaks also become broader with the increase of the propagation distance due to the strong self-phase modulation effect.

It should be noted that the above phenomena are not limited to only a fixed width of the quantum well. If, with a small change in the well width (from 32.9 a.u. to 31.8 a.u.; the corresponding transition frequency changes from $\omega_{12} = 1.11\omega_0$ to $1.18\omega_0$), the small-mismatch condition is still satisfied, similar phenomena should be expected. This hypothesis turns out to be correct, and the results are shown in Fig. 5.

By further reducing the quantum well width to 26.5 a.u., the transition frequency ω_{12} becomes $1.7\omega_0$, and therefore the frequency mismatch becomes quite large. Under larger-frequency mismatch, as shown in Fig. 6, even here for the spatially homogenous field case, only clearly odd-order harmonics (1, 3, 5, ...) dominate, which is linked to the rapid level crossing mechanism [42,43]. With the spatial inhomogeneity introduced, the harmonic-order character has no change. Only odd-order harmonics still remain, increasing the spatial inhomogeneity even further. However, the

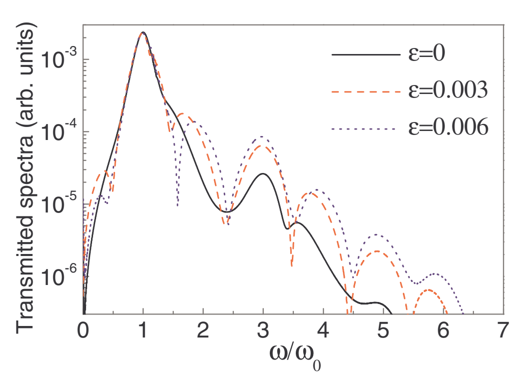

FIG. 5. (Color online) Same as in Fig. 2, but the well width is 31.8 a.u.

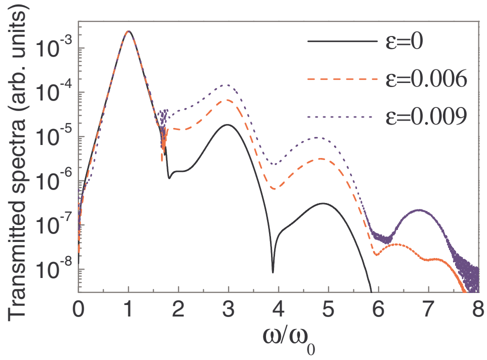

FIG. 6. (Color online) Same as in Fig. 2, but for a well width of 26.5 a.u.

higher spectral peaks increase obviously when the spatial inhomogeneity is included (dashed and dotted lines in Fig. 6), and even the seventh-order harmonic occurs for $\varepsilon = 0.006$ and becomes more clear at $\varepsilon = 0.009$. The reason can be found by investigating the time evolution of the laser field and the carrier-wave Rabi flopping, as done above. As indicated in Fig. 7(a), the spatially inhomogeneous laser field shows almost no obvious difference compared with that for the homogenous case. The corresponding population inversions shown in Fig. 7(b) are synchronous in both cases, which is quite different from those in Fig. 3(b). Increasing only the population inversions results directly in the intensity enhancement in the higher spectral components, as shown in Fig. 6.

The results in Figs. 2, 5, and 6 clearly indicate that the physical dynamics is quite different for different quantum well widths. This point is important for the potential applications for subwavelength optical devices.

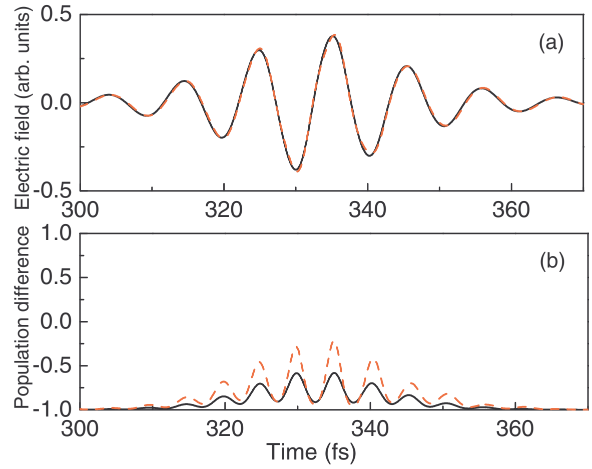

FIG. 7. (Color online) Same as in Fig. 3, but for a well width of 26.5 a.u.

IV. CONCLUSIONS

In conclusion, the propagation of a spatially inhomogeneous few-cycle laser field, linked to the surface plasmon polariton, through an ensemble of quantum wells has been studied. The influence of the spatial inhomogeneity and the propagation effect on the transmitted spectra distribution has been investigated in detail. The results show that the transmitted spectra sensitively depend on the spatial inhomogeneity due to the nonlinear propagation effects. Under the small-frequency mismatch condition satisfied by changing the quantum well width, for the spatially homogeneous case, the transmitted spectral distribution is almost continuous; however, if the spatial inhomogeneity is introduced, the spectral distribution becomes discrete, with clearly even- and odd-order harmonic peaks coexisting. These results can be explained in terms of the strong-field reshaping due to the propagation effect and the inversion symmetry breaking due to the introduction of the spatially inhomogeneous field. As for the case of large-frequency mismatch, only odd-order harmonics exist, no matter how strong the spatial inhomogeneity is. Moreover, in both cases of small- and large-frequency mismatch, the propagation effect can obviously enhance the intensity of the higher spectral components.

ACKNOWLEDGMENTS

This work is supported by the National Basic Research Program of China (Grant No. 2011CB808102) and the National Natural Science Foundation of China (Grants No. 11134010, No. 11374318, and No. 61008061). C.Z. gratefully acknowledges the support of a China Postdoctoral Science Foundation funded project (2013T60467) and the Qing Lan Project of Jiangsu Province. C.P.L. acknowledges the support from the 100-talents project of the Chinese Academy of Sciences.

[1] T. Brabec and F. Krausz, Rev. Mod. Phys. **72**, 545 (2000).
[2] Y. Zheng, Z. Zeng, P. Zou, L. Zhang, X. Li, P. Liu, R. Li, and Z. Xu, Phys. Rev. Lett. **103**, 043904 (2009).
[3] Z. Zeng, Y. Cheng, X. Song, R. Li, and Z. Xu, Phys. Rev. Lett. **98**, 203901 (2007).
[4] S. Hughes, Phys. Rev. Lett. **81**, 3363 (1998).
[5] O. D. Mücke, T. Tritschler, M. Wegener, U. Morgner, and F. X. Kärtner, Phys. Rev. Lett. **87**, 057401 (2001).
[6] T. Tritschler, O. D. Mücke, M. Wegener, U. Morgner, and F. X. Kärtner, Phys. Rev. Lett. **90**, 217404 (2003).
[7] C. Zhang, X. Song, W. Yang, and Z. Xu, Opt. Express **16**, 1487 (2008).
[8] X. Song, S. Gong, S. Jin, and Z. Xu, Phys. Rev. A **69**, 015801 (2004).
[9] W. Yang, S. Gong, and Z. Xu, Opt. Express **14**, 7216 (2006).
[10] N. Cui and M. A. Macovei, New J. Phys. **14**, 093031 (2012).
[11] C. Zhang, W. Yang, X. Song, and Z. Xu, J. Phys. B **42**, 125604 (2009).
[12] A. Husakou, S.-J. Im, and J. Herrmann, Phys. Rev. A **83**, 043839 (2011).
[13] I. Yavuz, E. A. Bleda, Z. Altun, and T. Topcu, Phys. Rev. A **85**, 013416 (2012).
[14] M. F. Ciappina, J. Biegert, R. Quidant, and M. Lewenstein, Phys. Rev. A **85**, 033828 (2012).

[15] M. F. Ciappina, S. S. Aćimović, T. Shaaran, J. Biegert, R. Quidant, and M. Lewenstein, Opt. Express **20**, 26261 (2012).
[16] T. Shaaran, M. F. Ciappina, and M. Lewenstein, Phys. Rev. A **86**, 023408 (2012).
[17] T. Shaaran, M. F. Ciappina, and M. Lewenstein, J. Mod. Opt. **59**, 1634 (2012).
[18] J. A. Pérez-Hernández, M. F. Ciappina, M. Lewenstein, L. Roso, and A. Zaïr, Phys. Rev. Lett. **110**, 053001 (2013).
[19] I. Yavuz, Phys. Rev. A **87**, 053815 (2013).
[20] M. F. Ciappina, T. Shaaran, and M. Lewenstein, Ann. Phys. (Berlin, Ger.) **525**, 97 (2013).
[21] B. Fetić, K. Kalajdžić, and D. B. Milošević, Ann. Phys. (Berlin, Ger.) **525**, 107 (2013).
[22] J. Luo, Y. Li, Z. Wang, Q. Zhang, and P. Lu, J. Phys. B **46**, 145602 (2013).
[23] S. Kim, J. Jin, Y.-J. Kim, I. -Y. Park, Y. Kim, and S.-W. Kim, Nature (London) **453**, 757 (2008).
[24] M. Sivis, M. Duwe, B. Abel, and C. Ropers, Nature (London) **485**, E1 (2012).
[25] S. Kim, J. Jin, Y.-J. Kim, I.-Y. Park, Y. Kim, and S.-W. Kim, Nature (London) **485**, E2 (2012).
[26] I.-Y. Park, S. Kim, J. Choi, D.-H. Lee, Y.-J. Kim, M. F. Kling, M. I. Stockman, and S.-W. Kim, Nat. Photonics **5**, 677 (2011).
[27] M. F. Ciappina, J. A. Pérez-Hernández, T. Shaaran, J. Biegert, R. Quidant, and M. Lewenstein, Phys. Rev. A **86**, 023413 (2012).
[28] T. Shaaran, M. F. Ciappina, and M. Lewenstein, Phys. Rev. A **87**, 053415 (2013).
[29] M. F. Ciappina, J. A. Pérez-Hernández, T. Shaaran, L. Roso, and M. Lewenstein, Phys. Rev. A **87**, 063833 (2013).
[30] W. Yang, X. Song, S. Gong, Y. Cheng, and Z. Xu, Phys. Rev. Lett. **99**, 133602 (2007).
[31] C. Van Vlack and S. Hughes, Phys. Rev. Lett. **98**, 167404 (2007).
[32] C. Zhang, Z. Wang, and B. Zhao, Phys. Lett. A **376**, 418 (2012).
[33] C. W. Luo, K. Reimann, M. Woerner, T. Elsaesser, R. Hey, and K. H. Ploog, Phys. Rev. Lett. **92**, 047402 (2004).
[34] X. Song, W. Yang, Z. Zeng, R. Li, and Z. Xu, Phys. Rev. A **82**, 053821 (2010).
[35] R. W. Ziolkowski, J. M. Arnold, and D. M. Gogny, Phys. Rev. A **52**, 3082 (1995).
[36] W. Yang, X. Song, R. Li, and Z. Xu, Phys. Rev. A **78**, 023836 (2008).
[37] V. P. Kalosha and J. Herrmann, Phys. Rev. Lett. **83**, 544 (1999).
[38] J. Xiao, Z. Wang, and Z. Xu, Phys. Rev. A **65**, 031402(R) (2002).
[39] C. Zhang, W. Yang, X. Song, and Z. Xu, Opt. Express **17**, 21754 (2009).
[40] C. Zhang, W. Yang, X. Song, and Z. Xu, Phys. Rev. A **79**, 043823 (2009).
[41] K. Yee, IEEE Trans. Antennas Propag. **14**, 302 (1966).
[42] F. I. Gauthey, C. H. Keitel, P. L. Knight, and A. Maquet, Phys. Rev. A **52**, 525 (1995), and references therein.
[43] C. P. Liu, S. Q. Gong, R. X. Li, and Z. Z. Xu, Phys. Rev. A **69**, 023406 (2004).